Int. J. Multiphase Flow Vol. 17, No. 3, pp. 343–354, 1991
Printed in Great Britain.

0301-9322/91 $3.00 + 0.00

EXPERIMENTS ON THE UNSTEADY DRAG AND WAKE OF A SPHERE AT HIGH REYNOLDS NUMBERS

Y. TSUJI, N. KATO and T. TANAKA
Faculty of Engineering, Osaka University, Suita, Osaka 565, Japan

(Received 22 July 1989; in revised form 12 October 1990)

Abstract—Drag on a sphere and its wake in a periodically pulsating flow were investigated experimentally. Measurements were made at Reynolds numbers in the range $8000 < Re < 16{,}000$. Results showed that the flow acceleration increases the drag as the existing theories for inviscid and low Re flows indicate. Quantitatively, the present drag data agree with the empirical formula given by Odar [*J. Fluid Mech.* **25**, 591–592 (1966)], although the Re which Odar's formula uses is much lower than those used here. It was found that the wake region is wider and the turbulent intensity in the wake is stronger during the period of deceleration than during acceleration.

Key Words: drag, unsteady wake

1. INTRODUCTION

The fluid drag on a particle, which is regarded as a classical subject in fluid dynamics, is the most important force when considering the mechanics of multiphase flows. In the analysis of multiphase flows, the particle shape is often assumed to be spherical for simplicity and the drag on a sphere is thought to have been well-understood. However, if effects like rotation, free-stream turbulence and unsteadiness are added to the problem, our understanding is still fragmentary, especially at high Reynolds numbers (Re). Lack of data for high Re under various conditions is seen in the monograph by Clift *et al.* (1978). All the effects mentioned above are important when considering the motion of large particles in many industrial flows. The authors have concentrated on the effects of unsteadiness in the present work, because two opposing results have been reported so far. One indicates that flow acceleration increases the drag, while the other suggests that flow deceleration increases the drag. Several reasons are considered for this qualitative difference, i.e. the experimental conditions such as the range of Re, the nature of unsteadiness and measuring methods. However, the relation between the different results and these conditions is unclear. The purpose of the present work is to offer a set of data obtained under different experimental conditions from previous works. It is beyond this work to clarify the relation of various factors and unsteady drag, because our data as well as previous data are still limited. The present study is in the process of accumulating data in a confused situation, as mentioned above. Below, previous studies concerning the effect of unsteadiness on the drag are briefly reviewed.

As is well-known, the drag F_D on a sphere at low Re numbers can be given theoretically:

$$F_D = 3\pi\mu D U_R + \frac{1}{2}\frac{\pi}{6}D^3\rho\frac{dU_r}{dt} + 6\frac{D^2}{4}\sqrt{\pi\rho\mu}\int_{t_0}^{t}\frac{\dfrac{dU_r}{dt}}{\sqrt{t-t'}}dt', \qquad [1]$$

where the first term on the r.h.s. is the Stokes drag, the second the added-mass term and the third the Basset history term. In [1], μ and ρ are fluid viscosity and density, D is the diameter of the sphere, U_r is the sphere velocity relative to the fluid and t_0 is the reference time. In this paper the Re is based on the sphere diameter D and the relative velocity U_r and the low Re is defined as the one for which the "creeping flow" approximation is applicable. The above equation has been established and widely used for studies of the motion of small particles in a fluid. Unfortunately, no theoretical expression is available for the drag at Re values higher than that of creeping flow. Thus, the drag at higher Re was investigated experimentally by some researchers. Among them, Odar & Hamilton's (1964) work is known for its precise measurements. They were the first to succeed in obtaining these three terms separately. In their experiment, the drag on a sphere

oscillating in an oil tank was measured at Re values up to 62. In this range of Re, it is considered that the sphere does not shed vortices, though it has a recirculating region behind it. The Re corresponding to the recirculating region is called the "intermediate Re" in this paper. They expressed the drag by the use of the empirical coefficients C_{Ds}, C_A and C_H:

$$F_D = C_{Ds}\frac{\pi}{4}D^2\tfrac{1}{2}\rho U_r^2 + C_A\frac{\pi}{6}D^3\rho\frac{dU_R}{dt} + C_H\frac{D^2}{4}\sqrt{\pi\rho\mu}\int_{t_0}^{t}\frac{\dfrac{dU_r}{dt}}{\sqrt{t-t'}}dt', \qquad [2]$$

where C_{Ds}, C_A and C_H are, respectively, the steady-state, added-mass and history drag coefficients. Based on their measurements, Odar (1966) gave the following empirical formulas for C_A and C_H:

$$C_A = 1.05 - \frac{0.066A_n^2}{1+0.12A_n^2}, \qquad C_H = 2.88 + \frac{3.12A_n^3}{(1+A_n)^3}; \qquad [3]$$

A_n is the acceleration factor defined by

$$A_n = \frac{D}{U_r^2}\frac{dU_r}{dt}. \qquad [4]$$

(In their original paper, a parameter which is the reciprocal of A_n is used in place of A_n.) Odar (1966) confirmed that [3], which was derived for a simple harmonic motion, is valid for the free fall of a sphere in a viscous fluid. The results of Odar & Hamilton (1964) and Odar (1966) show that the effect of unsteadiness is qualitatively the same as the existing theories which are obtained for inviscid and creeping flows.

Karanfilian & Kotas (1978) conducted a similar experiment using an oscillating sphere in a water or oil tank like Odar & Hamilton (1964). Their experiment was made at Re in the range $100 < \mathrm{Re} < 10{,}000$. They gave the following empirical values for the coefficients C_A and C_H:

$$C_A = 0.5, \qquad C_H = 6.0. \qquad [5]$$

These values are the same as [1] for the creeping flow regime. Karanfilian & Kotas (1978) described that the data arrangement based on the added-mass term and the history term causes a great deal of scatter. Therefore, they used the other formulation as well. That is, all the effects of unsteadiness are contained in the drag coefficient C_D, defined by

$$F_D = C_D\frac{\pi}{4}D^2\tfrac{1}{2}\rho U_r^2 \qquad [6]$$

where F_D is the instantaneous drag. They gave the following empirical expression for C_D:

$$C_D = (A_n+1)^{1.2}C_{Ds}, \qquad [7]$$

where C_{Ds} is the drag coefficient for the stationary flow ($A_n = 0$).

The experiments of Odar & Hamilton (1964) and Karanfilian & Kotas (1978) indicate that the drag at intermediate or high Re increases due to the acceleration of the relative velocity U_r. Contrary to the above, there is another group of works showing the opposite result. For instance, Temkin & Kim (1980) and Temkin & Mehta (1982) obtained the drag by observing the motion of spheres in a shock tube. In their formulation, all the effects of unsteadiness are contained in the drag coefficient C_D. They gave the following expression for the drag coefficient for Re = 9 to 115:

$$\left.\begin{aligned} C_D &= C_{Ds} - 0.048A_c \qquad (-45 < A_c < 3) \\ C_D &= C_{Ds} - \frac{3.829}{A_c} - 0.204 \qquad (5.9 < A_c < 25). \end{aligned}\right\} \qquad [8]$$

The parameter A_c is defined by

$$A_c = \left(\frac{\rho_p}{\rho} - 1\right)\frac{D}{U_r^2}\frac{dU_r}{dt}, \qquad [9]$$

where ρ_p is the particle (sphere) density. The above relation shows that the drag decreases due to the flow acceleration. Besides Temkin & Kim (1980) and Temkin & Mehta (1982), Ingebo (1956) reported a result showing the same trend. Temkin & Kim (1980) and Temkin & Mehta (1982) attributed the differences between their drag results and the stationary drag to the change in the recirculating region in the rear of the sphere. That is, the recirculating region of a sphere is considered to become smaller in the accelerating flow, and this is related to smaller drag. It is noted that the range of Re in the experiments of Temkin & Kim (1980) and Temkin & Mehta (1982) is almost the same as that in the experiment of Odar & Hamilton (1964). Therefore, the difference in results is considered to come from the nature and degree of unsteadiness.

Marchildon & Gauvin (1979) conducted a free fall test of a sphere in still air and drew the conclusion that deceleration increases the drag. They described that their data indicated no apparent effect of acceleration within their experimental conditions. Their Re range overlaps the present range and the experiment was made in gas. However, it should be noted that there is a difference between their experiment and the present one. That is, in a free fall test, particle motion and drag are affected by vortex shedding. The effect of vortex shedding on the particle motion is clearly shown by Schoeneborn (1975). The influence of vortex shedding is manifested when the particle/fluid density ratio is small.

In most experiments of unsteady drag at high Re, unsteady flow conditions were produced by oscillation of a sphere in a fluid tank, by a free fall test of a sphere or by the stepwise change in fluid velocity in a shock tube. In the present work, the unsteady flow was produced in a wind tunnel, where a large oscillating flow was superimposed on a uniform stream. A sphere was fixed in the periodically changing flow. This experimental method is convenient for investigating the relation between the drag and the velocity field behind the sphere, because the wake of the sphere is easy to measure together with the drag measurement.

2. EXPERIMENTAL FACILITIES AND PROCEDURE

2.1. Pulsating flow generator

The wind tunnel used in the present experiment is shown in figure 1. The test section has the following dimensions: 450 mm high, 600 mm wide and 800 mm long. The width of the tunnel after the test section is contracted from 600 to 200 mm. A flat plate is set up at the outlet of the tunnel, having a fixed gap with the end of the tunnel. Pulsating flow is produced by using a cam mechanism attached to the plate and changing the gap between the plate and the exit, as shown in figure 2. The air velocity was measured by a single hot-wire probe, and thus only the longitudinal component u was measured. Figure 3 presents the instantaneous velocity obtained at the highest frequency in this facility. The authors tried to increase the amplitude and frequency of the flow oscillation as much as possible to see the effects of acceleration clearly. However, if the amplitude and frequency are made too large, the wave form of the instantaneous air velocity is distorted from the sinusoidal wave. The sinusoidal wave form is necessary to estimate the Basset term, as explained in the appendix. From these conditions the range of acceleration shown in table 1 is determined.

Since the present experiment is related to separation on the sphere, the free-stream turbulence is an important parameter. The turbulence intensities $(\overline{u'^2})^{1/2}/U$ in the free stream were measured in both steady and pulsating flows, where u' is the fluctuating component of the fluid velocity and

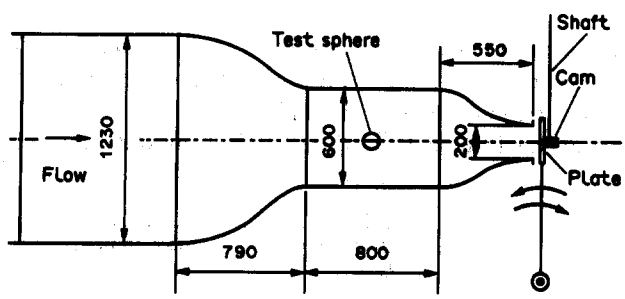

Figure 1. Wind tunnel.

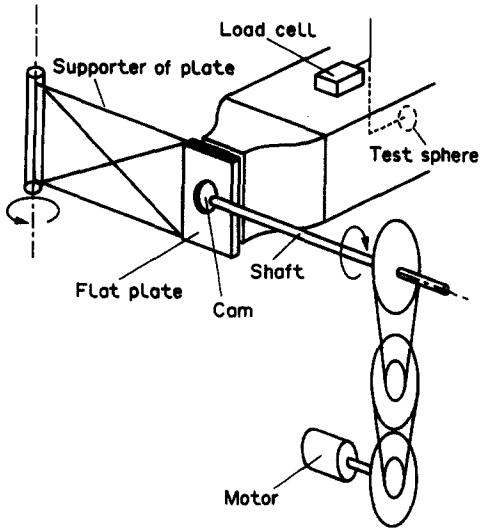

Figure 2. Pulsating flow generator.

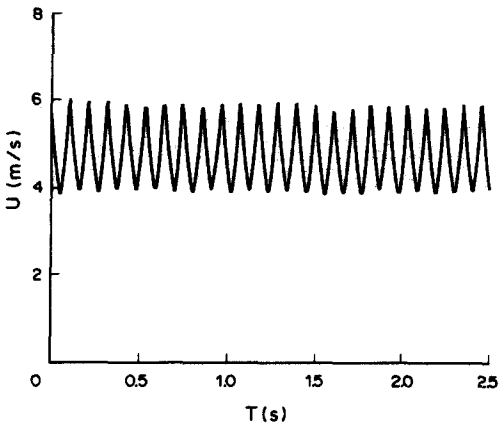

Figure 3. Wave form of the free-stream velocity ($f = 10$ Hz).

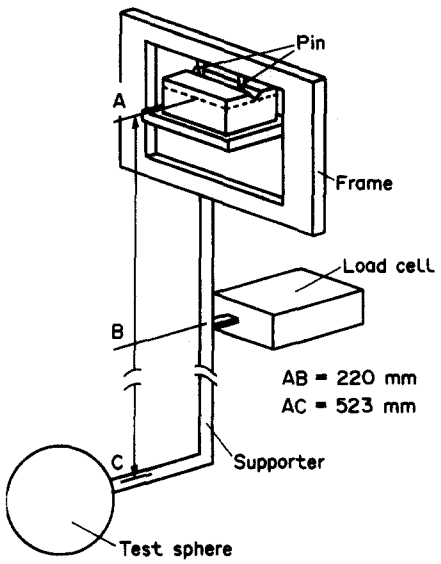

Figure 4. Equipment for measuring the drag force.

U is the mean free-stream velocity. In the steady flow it was about 0.01. In the pulsating flow, the turbulence intensity in the free stream was measured by the same method as described in section 4, i.e. the phases of 0° and 180° in figure 13 were chosen as representative of the accelerating and decelerating flows, and the standard deviation based on the ensemble average was calculated from digitized signals. The intensity thus obtained ranged from 0.013 to 0.015.

2.2. Measurement of drag

The device for drag measurement is shown in figure 4. The test sphere, which was a table tennis ball, 37.38 mm dia and 2.5 g in weight, was supported by an L-type wooden rod (12 × 6 mm). The rod was covered with a hood to negate the influence of the flow. The top of the rod was supported by a pin joint, and a lever extending from the rod was connected to a load cell for

Table 1. Experimental conditions

Air velocity, U(m/s)	Pulsation frequency, f(Hz)	Reynolds number, (Re)	Acceleration, dU/dt(m/s)	Acceleration factor, A_n
3 to 6	2.5 to 8	8000 to 16,000	−40 to 40	−0.08 to 0.08

small force. The drag force was amplified by a factor of AC/AB, and detected by the load cell. The problem encountered in this kind of measurement is that of natural oscillation, the characteristic frequency of which is inherent to the supporting system. In order to prevent the drag measurement from being affected by such oscillation, the characteristic frequency should be as large as possible, and therefore light and hard materials were used as the sphere and supporter. In the present experiment, the frequency of the natural oscillation was 52 Hz. As far as we could see with the naked eye, no oscillation of the sphere and supporter was observed during the experiment.

2.3. Data processing

Signals from the hot-wire anemometer and the load cell were processed by a personal computer (NEC 9800VM) following an A/D converter. The digitizing rate was 500 Hz. Figure 5 shows wave forms of the instantaneous air velocity in the main stream and the force detected by the load cell. The air velocity shows a desirable pattern, but the force contains fluctuation of a higher frequency which is caused by the characteristic oscillation of the present supporting system. If such draft signals showing large fluctuations are used as they are, data scatter too much to see any signs of the effects of unsteadiness. Therefore, the signals were smoothed by using the following averaging techniques.

In the present work, two methods of averaging were used: the moving average and the ensemble average. The method of the moving average is well-known as a method taking a low-frequency component from a wave accompanied by an irregular high-frequency component. In the moving average, the value at a certain instant is obtained by averaging several sequential values near the instant of interest. The number of instants for averaging is fixed. For example, if 5 instants are chosen before and 5 after the instant of interest, the number of instants for averaging becomes 11 in all, and therefore the value of the moving average is obtained from the following equation:

$$F_i = \frac{\sum_{k=-5}^{5} F_{i+k}}{11}. \qquad [10]$$

(The time interval between sequential instants is 0.002 s.) This averaging calculation is made along the time axis. Figure 6 shows the wave forms obtained from figure 5 by using [10]. It is found that fluctuation of higher frequency is remarkably reduced. In the present work, the wave forms were further smoothed by taking the ensemble average on 30–100 wave forms which were already processed by the moving average. Figure 7 shows the final wave forms, which are adopted in this work as the instantaneous drag force on the sphere.

Table 1 shows the present experimental conditions. The ranges of Re and frequency in the present experiment are automatically determined by restrictions imposed on the equipment, like the size of the measuring section of the wind tunnel used and the characteristic oscillation of the supporting system of the sphere.

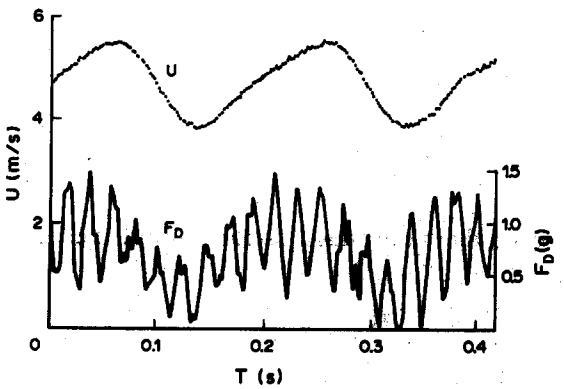

Figure 5. Wave forms of the free-stream velocity and drag.

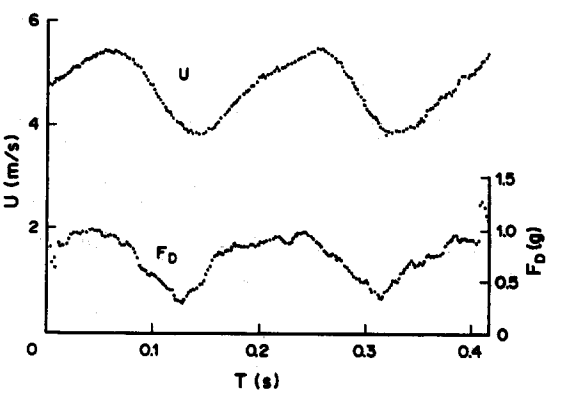

Figure 6. Wave forms after the moving average method.

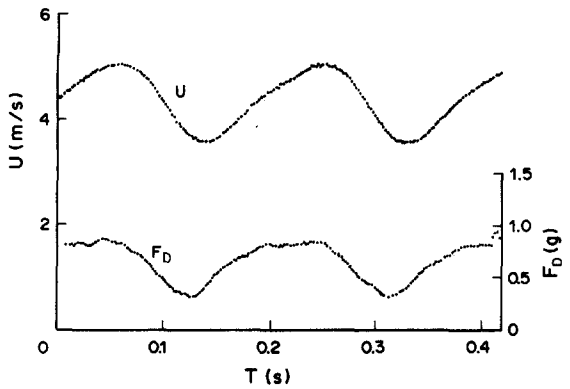

Figure 7. Wave forms after the ensemble average method.

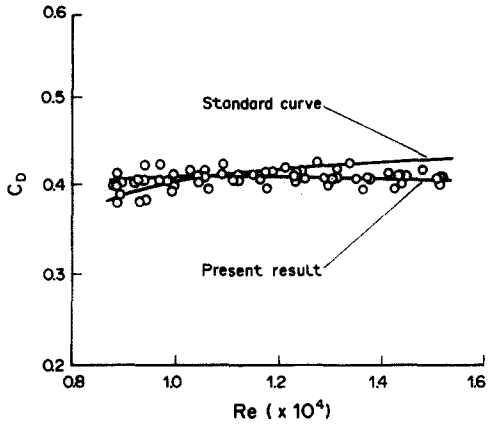

Figure 8. Drag coefficient C_D vs Re in steady flow.

3. DRAG

Following Temkin & Kim (1980) and Temkin & Mehta (1982), the present authors let the drag coefficient C_D contain all the contributions of unsteadiness. The drag coefficient C_{Ds} measured in the steady flow is shown in figure 8, where the standard curve is also presented for comparison. It is found that reasonably good agreement is obtained for the steady-state drag. The slight difference from the standard curve is caused by the supporting system used in this experiment. Regarding the presentation of the unsteady results, two forms are adopted in this paper: one is the relation between C_D and instantaneous Re, and the other is the relation between the difference $C_D - C_{Ds}$ and the acceleration factor A_n.

Figures 9(a–e) show the results of C_D vs Re for different pulsating frequencies. The plotted points were obtained from data of two cycles of pulsation. The dark points correspond to flow acceleration, and the solid line represents the result of stationary drag. It is clear from the figures that flow acceleration increases the drag, and that the higher the frequency, the larger the deviation from the stationary drag curve. This result is qualitatively the same as the existing theories obtained for inviscid and creeping flows and contrary to the experimental results of Temkin & Kim (1980) and Temkin & Mehta (1982).

The results of $(C_D - C_{Ds})$ vs A_n, corresponding to figures 9(a–e), are shown in figures 10(a–e), it is found from the figures that the relation of $(C_D - C_{Ds})$ vs A_n is expressed approximately by a straight line.

Next, the present results are compared with the empirical expression of Odar (1966). For such a comparison, the pressure gradient term should be added to [2], because in a pulsating flow such as the present one the force due to the pressure gradient acts on the sphere in addition to the steady-state, added-mass and history terms. Therefore, for the present case,

$$F_D = C_{Ds}\frac{\pi}{4}D^2\tfrac{1}{2}\rho U_r^2 - \frac{\pi}{6}D^3\frac{dp}{dx} + C_A\frac{\pi}{6}D^3\rho\frac{dU_r}{dt} + C_H\frac{D^2}{4}\sqrt{\pi\rho\mu}\int_{t_0}^{t}\frac{\dfrac{dU_r}{dt}}{\sqrt{t-t'}}dt', \quad [11]$$

where $U = U_r$ because the present sphere is fixed. Assuming that the fluid is incompressible, the pressure gradient in the free stream is related to the velocity U by the equation of fluid motion:

$$\frac{dU}{dt} = -\frac{1}{\rho}\frac{dp}{dx}. \quad [12]$$

Substituting [12] into [11] and using the definition of the acceleration factor [4] and the drag coefficient C_D [6], we obtain

$$C_D = C_{Ds} + \tfrac{4}{3}(1 + C_A)A_n + C_H\frac{\sqrt{\dfrac{\rho\mu}{\pi}}}{\frac{1}{2}\rho U^2}\int_{t_0}^{t}\frac{\dfrac{dU_r}{dt}}{\sqrt{t-t'}}dt'. \quad [13]$$

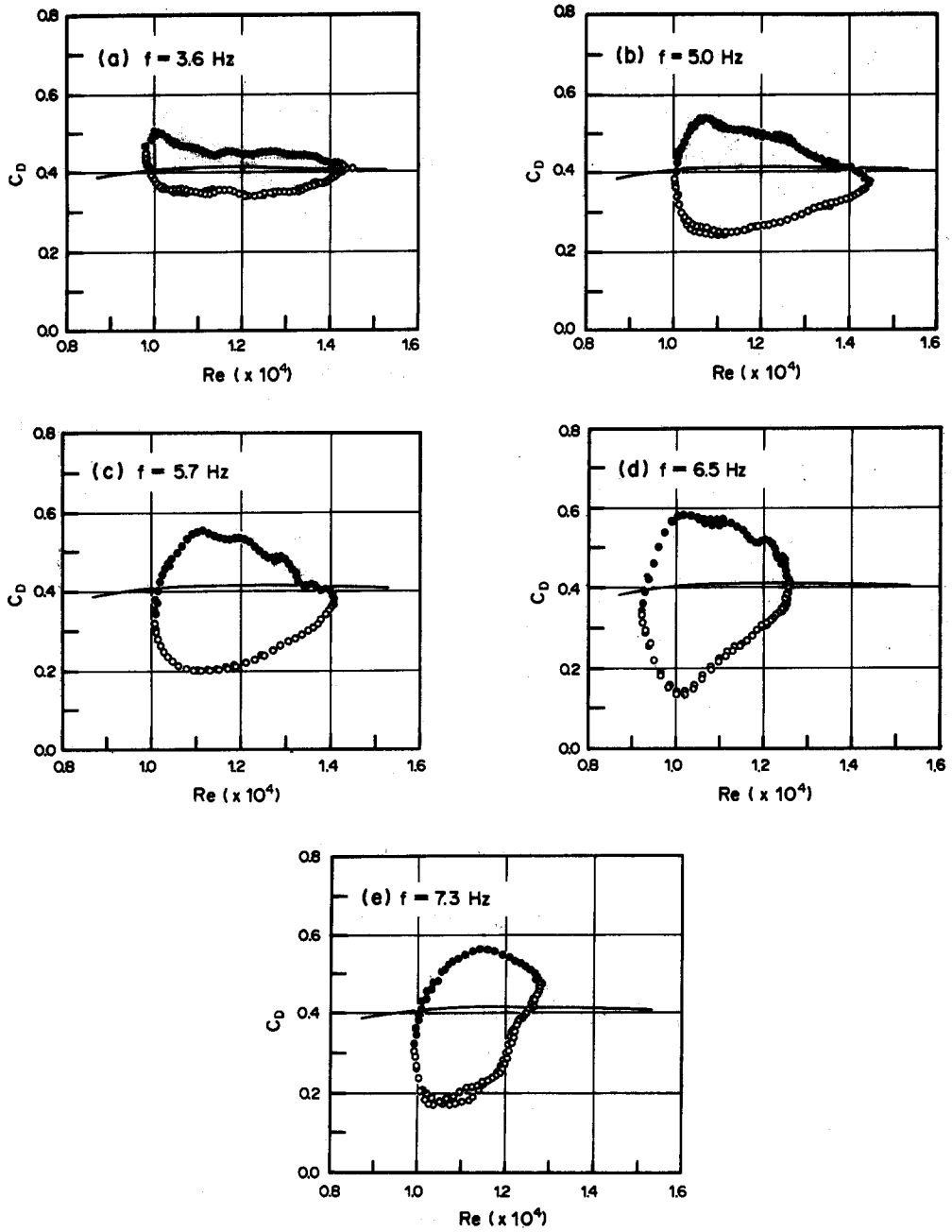

Figure 9. Drag coefficient C_D vs Re in unsteady flow. ——, Standard drag curve; ●, accelerating flow; ○, decelerating flow. (a) $f = 3.6$ Hz; (b) $f = 5.0$ Hz; (c) $f = 5.7$ Hz; (d) $f = 6.5$ Hz; (e) $f = 7.3$ Hz.

If the history term (the third term on the r.h.s.) is neglected, we obtain

$$C_D - C_{Ds} = \tfrac{4}{3}(1 + C_A)A_n. \qquad [14]$$

The magnitude of the history term is estimated in the appendix and it is shown that it can be neglected under the present conditions.

The linear relation between $(C_D - C_{Ds})$ and A_n shown in figures 10(a–e) corresponds to C_A being constant in [14]. This is one of the findings of the present work. This finding is not surprising because coefficients appearing in the non-dimensionalizing process based on the dynamic pressure have a tendency to become constant at high Re, in general, e.g. the Newtonian drag coefficient and friction factor of the pipe flow at high Re. An unexpected finding is that the present value of C_A is the same as Odar (1966) gave for $Re < 62$, which is much smaller than the present Re.

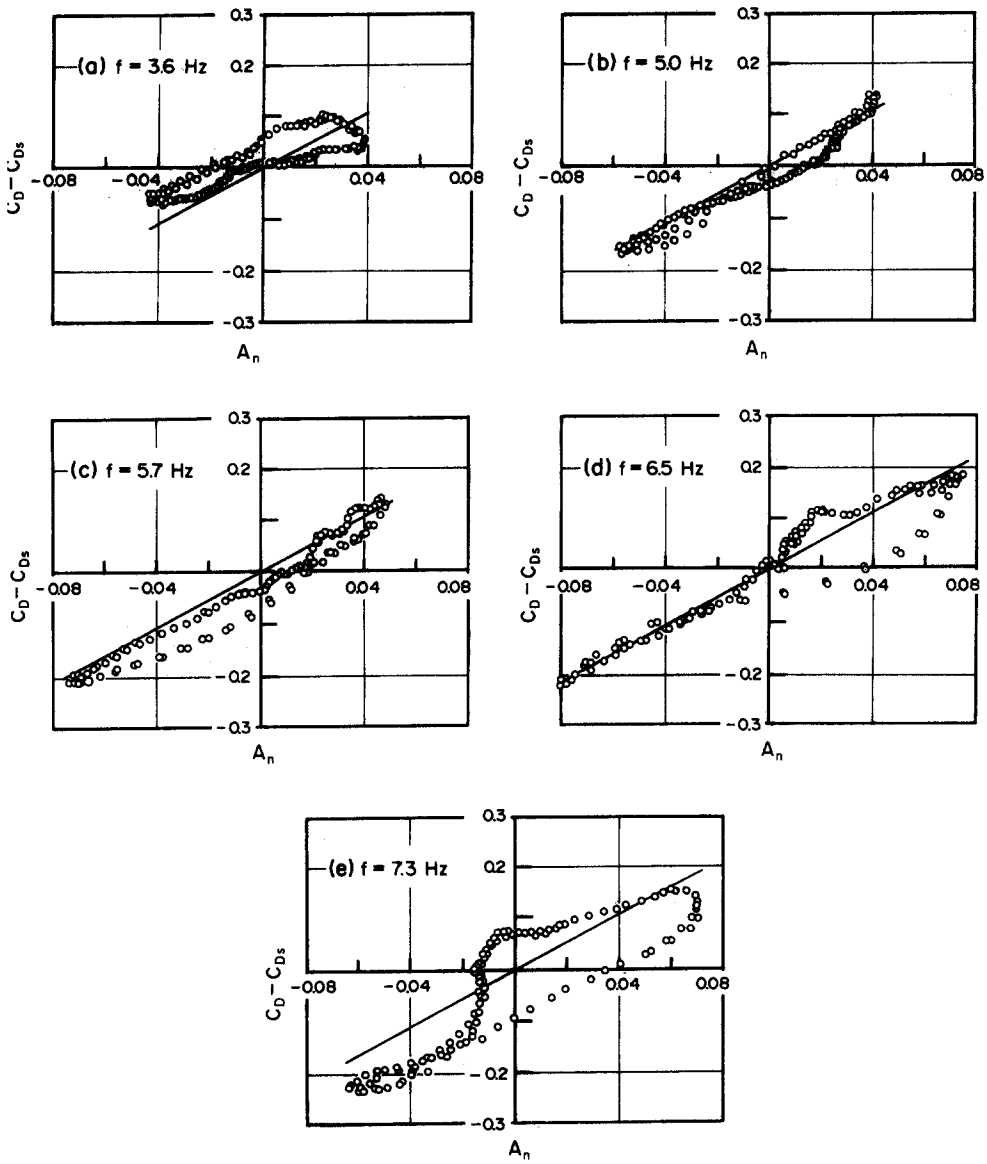

Figure 10. $(C_D - C_{Ds})$ vs A_n. ——, [16]. (a) $f = 3.6$ Hz; (b) $f = 5.0$ Hz; (c) $f = 5.7$ Hz; (d) $f = 6.5$ Hz; (e) $f = 7.3$ Hz.

In the present experimental condition, the absolute value of A_n is small, 0.08 at maximum. Therefore, neglecting the higher orders in [3]:

$$C_A = 1.05. \qquad [15]$$

Substituting the above value into [14]:

$$C_D - C_{Ds} = 2.7A_n. \qquad [16]$$

The inclined straight line in figures 10(a–e) is given by [16]. In figures 10(a–e), the range of A_n in [16] is taken according to the experimental values of A_n. It is seen in figures 10(a–e) that the present results show good agreement with [16]. In figure 10(e), the experimental results show a large loop. This loop is considered to be due to the history effect. However, detailed consideration of this loop is not undertaken in the present work. If the present measurements are compared with the results of Karanfilian & Kotas (1978) or with the theory for the low Re, the degree of agreement becomes worse, since the unsteady terms in such results are smaller than those of Odar (1966).

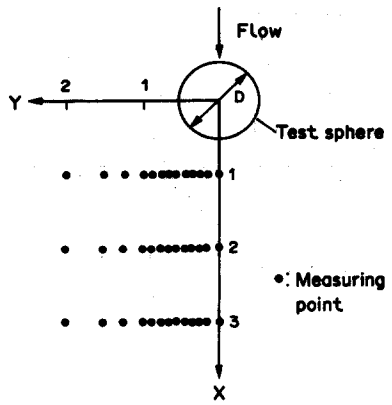

Figure 11. Measuring points on the wake.

4. WAKE

Figure 11 shows the measuring points of the wake and the coordinate system. The center of the sphere is taken as the origin of the coordinates X and Y. X is the stream-wise coordinate and Y is normal to X. The scale numbers for the coordinates denote the distance from the origin made dimensionless with the sphere diameter D. In the measurements of the wake, two hot-wire probes were used; one probe monitored the main stream and the other was traversed across the wake. The monitor probe was set up in the free stream in the plane of $X = 0$. Instantaneous velocity forms are shown in figures 12(a, b) where the dashed lines represent the velocity in the main stream. The results in figures 12(a, b) were obtained at the same point, but in steady (a) and unsteady (b) flow conditions. The position of $X = 2$ and $Y = 0.85$ is near the edge of the wake and thus the velocity shows intermittent turbulence. It is found from comparison of these two figures that the occurrence

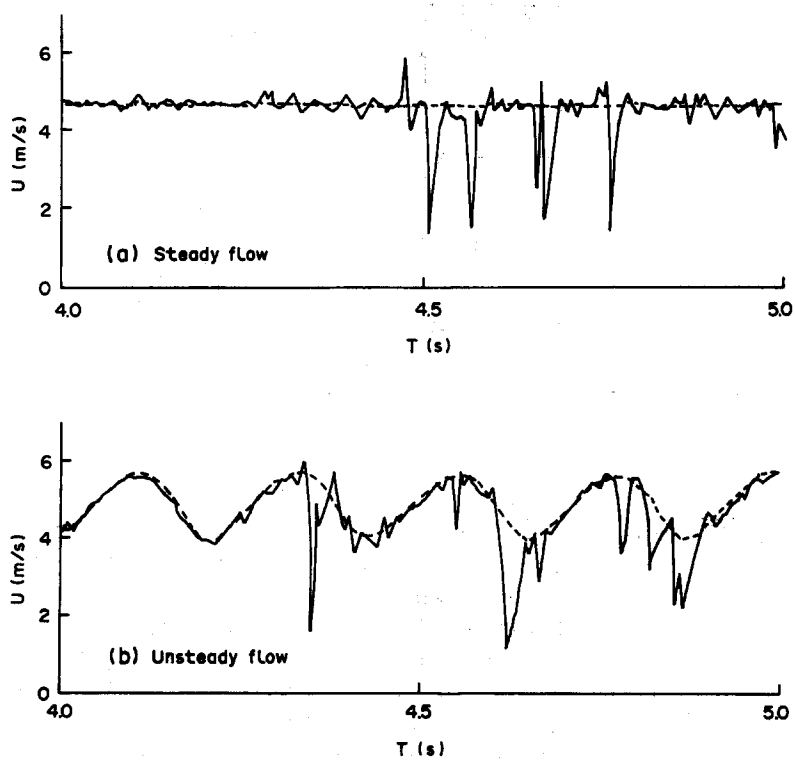

Figure 12. Instantaneous velocity signals; $X = 2$, $Y = 0.85$.

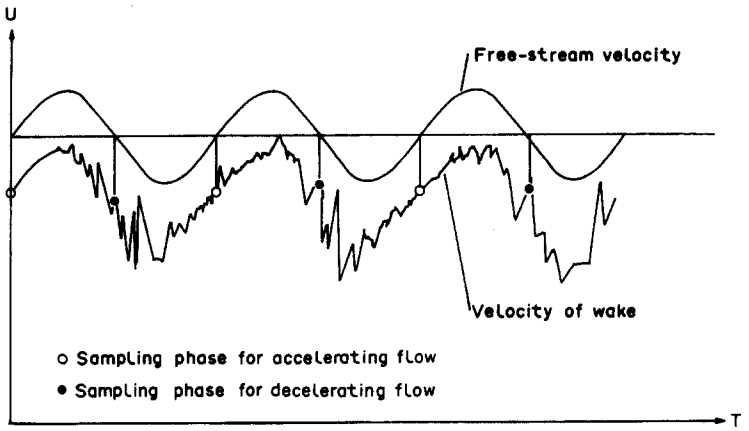

Figure 13. Phase in the velocity distribution measurements.

of turbulence is marked in the decelerating flow, while turbulence is scarcely observed in the accelerating flow.

The present authors attempted flow visualization of the wake by the smoke wire technique, but unfortunately instantaneous pictures indicate no apparent effect of unsteadiness, except for a slight increase in the width of the wake. Although the flow visualization gave little information, hot-wire measurements of the distributions of the mean velocity and turbulence intensity showed different tendencies between the periods of acceleration and deceleration. Distributions at a certain phase were obtained by collecting instantaneous values of velocity at the same phase. In this work, the phases of 0° and 180° in figure 13 were chosen as representative of the accelerating and decelerating flow conditions, respectively. The main stream velocity of the steady-state condition was adjusted to be the same as the time mean velocity of the unsteady flow $U = 4.6$ m/s. Figure 14 shows such distributions of the mean velocity and turbulence intensity across the stream. As expected from figures 12(a, b), the thickness of the wake is greatest in the decelerating flow. The thickness in the steady-state flow is between that in the accelerating and decelerating flows. Regarding the turbulence intensity near the centerline, the steady-state results show the largest values, and the case of acceleration shows the smallest intensities. The same results as in figure 14 were obtained at different frequencies.

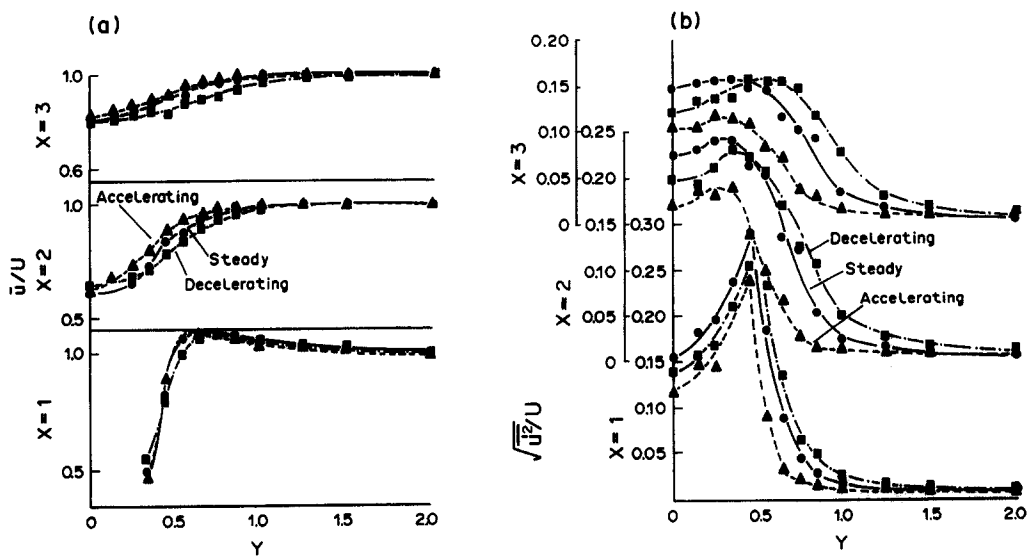

Figure 14. Distributions of mean velocity and turbulence intensity ($f = 3.5$ Hz). (a) Mean velocity; (b) turbulence intensity.

Table 2. Comparison of previous and present experimental conditions

Researchers	Fluid	Re	Maximum value of $\lvert A_n \rvert$
Odar & Hamilton (1964)	Liquid	0–62	3.7
Karanfilian & Kotas (1978)	Liquid	100–10,000	10.5
Temkin & Mehta (1982)	Gas	9–115	0.045
Temkin & Kim (1980)	Gas	3.2–77	0.040
Marchildon & Gauvin (1979)	Gas	1000–10,000	0.006
Present work	Gas	8000–16,000	0.08

5. DISCUSSION

Table 2 shows a comparison of the present experimental conditions with those of other researchers. The acceleration factor A_n is defined by [4]. In principle, the maximum value of A_n becomes infinite in the case of an oscillating sphere in a still fluid, as in the experiments of Karanfilian & Kotas (1978) and Marchildon & Gauvin (1979). The maximum values in such experiments, shown in table 2, are those which those authors used for constructing empirical formulas of the drag coefficient. Table 2 shows a characteristic feature of each experiment. As expected, the maximum value of A_n is much larger in experiments using oscillating spheres than in other experiments. Under the present conditions, the Re is high in general. Although the present maximum value of A_n is smaller than in the case of an oscillating sphere in liquid, it is larger than in other experiments in gas.

In general, the previous data showing that the drag increases due to flow deceleration was obtained from experiments in gas, while the opposite result was obtained from experiments in liquid. Although the present experiment was made in gas (air), the results support those obtained from experiments in liquid.

Since the present results are still limited, it is difficult to explain in full the reasons for the differences between the present results and other opposing results. However, it is safe to say that at high Re and with a relatively high acceleration rate, the effect of unsteadiness on the drag has the same trend as that established by existing theories for inviscid and creeping flows. Further, the quantitative agreement of the present results with the empirical formula of Odar (1966) is interesting. Odar's formula is based on experiments with $\mathrm{Re} < 62$. On the other hand, the range of the present Re is $8000 < \mathrm{Re} < 16{,}000$. When considering the difference in the drag mechanisms between these two cases, there is a possibility that the above agreement is a mere coincidence.

Another important result of this work is concerned with the relation between the drag and the wake. Although the wake changes due to the flow acceleration or deceleration, the drag does not change necessarily in the way expected from the change in wake.

6. CONCLUSION

The effects of flow unsteadiness on the drag and wake of a sphere have been investigated. A sphere (37.38 mm dia) was set up in a wind tunnel in which a periodically pulsating flow was produced. The Re range based on the sphere diameter and free-stream velocity was $8000 < \mathrm{Re} < 16{,}000$, and the frequency of pulsation ranged from 2.5 to 8 Hz. The degree of acceleration or deceleration was low in the present experiment, but the effects of unsteadiness were clearly observed. The results obtained are summarized as follows:

(1) The drag increases in the accelerating flow and decreases in the decelerating flow as indicated by the existing theories established for inviscid and creeping flows. Quantitatively, the present experimental results show good agreement with the empirical formula given by Odar (1966).
(2) In the intermittent region, the occurrence of turbulence is more marked in the decelerating flow than in the accelerating flow.
(3) The wake region becomes wider in the decelerating flow and smaller in the accelerating flow than in the steady flow.

Acknowledgements—The authors would like to acknowledge the continuing guidance and encouragement of Professor Y. Morikawa. The authors wish to thank Mr Y. Kawata and Mr Y Kayukawa for their assistance in the present experiment. The authors also wish to thank Dr M. Iguchi for helpful suggestions regarding the pulsating flow generator. This work was supported by a Grant-in-Aid for Scientific Research (No. 62550130) from the Ministry of Education, Science and Culture of Japan; this support is gratefully acknowledged.

REFERENCES

CLIFT, R., GRACE, J. R. & WEBER, M. E. 1978 *Bubbles, Drops, and Particles.* Academic Press, New York.

INGEBO, R. D. 1956 Drag coefficients for droplets and solid spheres in clouds accelerating in air streams. NACA Technical Note TN 3762.

KARANFILIAN, S. K. & KOTAS, T. J. 1978 Drag on a sphere in unsteady motion in a liquid at rest. *J. Fluid Mech.* **87,** 85–96.

MARCHILDON, E. K. & GAUVIN, W. H. 1979 Effects of acceleration, deceleration and particle shape on single-particle drag coefficient in still air. *AIChE Jl* **25,** 938–948.

ODAR, F. 1966 Verification on the proposed equation for calculation of the forces on a sphere accelerating in a viscous fluid. *J. Fluid Mech.* **25,** 591–592.

ODAR, F. & HAMILTON, W. S. 1964 Forces on a sphere accelerating in a viscous fluid. *J. Fluid Mech.* **18,** 302–314.

SCHOENEBORN, P. P. 1975 The interaction between a single particle and an oscillating fluid. *Int. J. Multiphase Flow* **2,** 307–317.

TEMKIN, S. & KIM, S. S. 1980 Droplet motion induced by weak shock waves. *J. Fluid Mech.* **96,** 133–157.

TEMKIN, S. & MEHTA, H. K. 1982 Droplet drag in an accelerating decelerating flow. *J. Fluid Mech.* **116,** 297–313.

APPENDIX

Order Estimate of the History Term and Derivation of [14]

In order to estimate the order of magnitude of the history term, the present pulsating flow is expressed approximately as the sum of a uniform flow and a harmonic motion, as in Odar & Hamilton (1964):

$$U = U_m = A_0 \sin 2\pi ft. \qquad [A.1]$$

Substituting this expression and $t_0 = -\infty$ for the third term in [13], we obtain

$$C_H \frac{\sqrt{\frac{\rho\mu}{\pi}}}{\frac{1}{2}\rho U^2} \int_{t_0}^{t} \frac{\frac{dU_r}{dt}}{\sqrt{t-t'}} dt' = C_H \frac{A_0\sqrt{4\pi fv}(\cos 2\pi ft + \sin 2\pi ft)}{U^2}. \qquad [A.2]$$

In the present experimental conditions, the absolute value of A_n is small, 0.08 at maximum. Therefore, neglecting the higher orders in [3]:

$$C_A = 1.05, \; C_H = 2.88. \qquad [A.3]$$

The order of magnitude of [A.2] estimated by the present data is $O(10^{-3})$. For instance, this can be confirmed by substituting the following values in [A.1]:

$$A_0 = 1 \text{ m/s}, \qquad U_m = 5 \text{ m/s}, \qquad f = 8 \text{ Hz}.$$

The above f is the maximum value in the present experimental conditions. The order of the other terms in [13] is $O(10^{-1})$. Therefore, the contribution of the history term can be neglected.